Tryptophan Mutants of Cardiac Troponin C: 3D Structure, Troponin I Affinity, and in Situ Activity † , ‡

ARTICLE *in* BIOCHEMISTRY · FEBRUARY 2008

Impact Factor: 3.02 · DOI: 10.1021/bi702056g · Source: PubMed

7 AUTHORS, INCLUDING:

Olivier Julien
University of California, San Francisco
22 PUBLICATIONS **144** CITATIONS
SEE PROFILE

Yin-Biao Sun
King's College London
46 PUBLICATIONS **802** CITATIONS
SEE PROFILE

Darrin A Lindhout
NGM Biopharmaceuticals, Inc.
19 PUBLICATIONS **403** CITATIONS
SEE PROFILE

Tryptophan Mutants of Cardiac Troponin C: 3D Structure, Troponin I Affinity, and *in Situ* Activity[†,‡]

Olivier Julien,[▽] Yin-Biao Sun,[§] Xu Wang,[▽] Darrin A. Lindhout,[▽] Angela Thiessen,[▽] Malcolm Irving,[§] and Brian D. Sykes*[,▽]

Department of Biochemistry, University of Alberta, Edmonton, Canada, Randall Division of Cell and Molecular Biophysics, King's College London, United Kingdom

Received October 12, 2007; Revised Manuscript Received November 13, 2007

ABSTRACT: *In situ* fluorescence/NMR spectroscopic approaches have been used to elucidate the structure, mobility, and domain orientations of troponin C in striated muscle. This led us to consider complementary approaches such as solid-state NMR spectroscopy. The biophysical properties of tryptophan and Trp-analogues, such as fluorotryptophan or hydroxytryptophan, are often exploited to probe protein structure and dynamics using solid-state NMR or fluorescence spectroscopy. We have characterized Phe-to-Trp mutants in the 'structural' C-domain of cardiac troponin C, designed to immobilize the indole ring in the hydrophobic core of the domain. The mutations and their fluorinated analogues (F104W, F104(5*f*W), F153W, and F153(5*f*W)) were shown not to perturb the structural properties of the protein. In this paper, we characterize the mutations F77W and F77W-V82A in the 'regulatory' N-domain of cardiac troponin C. We used NMR to determine the structure and dynamics of the mutant F77W-V82A-cNTnC, which shows a unique orientation of the indole ring. We observed a decrease in calcium binding affinity and a weaker affinity for the switch region of TnI for both mutants. We present force recovery measurements for all of the N- and C-domain mutants reconstituted into skeletal muscle fibers. The F77W mutation leads to a reduction of the *in situ* force recovery, whereas the C-domain mutants have the same activity as the wild type. These results suggest that the perturbations of the N-domain caused by the Trp mutation disturb the interaction between TnC and TnI, which in turn diminishes the activity in fibers, providing a clear example of the correlation between *in vitro* protein structures, their interactions, and the resulting *in situ* physiological activity.

Many, if not most, proteins exist as parts of large, complex biomacromolecular assemblies such as fibers, viruses, cell walls, nanomotors, and membrane surface receptors. One of the most studied of these systems is striated muscle, where structures of many important isolated components involved in force generation and calcium regulation have been determined. The wealth of troponin structures includes X-ray and NMR structures of the apo and calcium saturated versions of troponin C from skeletal and cardiac muscle (*1*−*6*), of troponin C in complex with fragments of the inhibitory target protein TnI[1] (*7*, *8*), and X-ray structures of the core regions of the skeletal and cardiac troponin complexes (*9*, *10*). These *in vitro* structures provide a detailed molecular description of many of the important interactions among the regulatory proteins. It is, however, very important but typically much more difficult to determine the structures of proteins in their native environments in order to elucidate the molecular details of their mechanism of action. One approach which has been exploited quite successfully in the motility area uses fluorescence spectroscopy of bifunctional rhodamine-labeled proteins to determine the *in situ* orientation of domains of proteins whose structures are known *in vitro*. This approach has been used to determine the orientations of the domains of the bilobal myosin regulatory light chain and troponin C proteins reconstituted into skeletal muscle fibers (*11*, *12*). This data has subsequently been used in combination with other studies such as cryoelectron microscopy to build detailed model structures positioning the major protein components in the intact muscle fiber (*13*, *14*).

The bifunctional rhodamine label is, however, a large, hydrophobic, and potentially mobile probe. We have sought to develop an intrinsic, more rigid, nonperturbing probe that might be used with either fluorescence or solid-state NMR spectroscopies. The spectroscopic properties of tryptophan as a probe are appropriate, and tryptophan is relatively scarce in proteins, so that single tryptophan mutants have been widely used in biophysical studies. These include the Trp

[†] Funded by the Canadian Institutes of Health Research and Canada Research Chairs. Y.-B.S. was supported by the British Heart Foundation (FS/04/083). O.J. is the recipient of Studentships from the Fonds de la Recherche en Santé du Québec (FRSQ) and the Alberta Heritage Foundation for Medical Research (AHFMR).

[‡] The Protein Data Bank code is 2jxl.

* To whom correspondence should be addressed. Telephone: +1-780-492-5460. Fax: +1-780-492-0886. E-mail: brian.sykes@ualberta.ca.

[▽] University of Alberta.

[§] King's College London.

[1] Abbreviations: TnC, troponin C; TnI, troponin I; cTnC, human cardiac troponin C; cNTnC, N-domain of cTnC; F77W-V82A, cTnC containing mutation Phe 77 to Trp and Val 82 to Ala; $cTnI_{147-163}$ or cSp, switch peptide of cTnI; 4*f*W, 4-fluorotryptophan; 5*f*W, 5-fluorotryptophan; TFE, trifluoroethanol; HSQC, heteronuclear single quantum coherence; NOE, nuclear Overhauser enhancement; K_d, dissociation constant for Ca^{2+} or cSp; K_{dimer}, dissociation constant for the formation of dimer.

10.1021/bi702056g CCC: $40.75
Published on Web 12/20/2007

F78W and F154W mutants of skeletal TnC, which are analogous to the mutants described herein (*15*), and many others (*15*−*17*) including the widely used F29W (*18*). In many cases, however, the design strategy was the opposite to ours: to have the largest spectroscopic change resulting from the large conformational change concomitant with calcium binding. Tryptophan analogues such as fluorotryptophan and hydroxytryptophan also have special spectroscopic properties that can be exploited using solid-state NMR (*19*) and fluorescence (*20*) spectroscopies, respectively. We have previously characterized two Phe-to-Trp mutants in the C-terminal domain of cTnC (*21*). The mutations were designed to immobilize the indole ring within the hydrophobic core of the EF-hand calcium binding domain, by replacing the phenylalanine residue anchoring the calcium binding loops of sites III and IV. These single mutants of cTnC and their fluorinated analogues (F104W, F104(5*f*W), F153W, and F153(5*f*W)) were shown to have very similar overall structures compared to the wild type protein with their indole ring immobilized (*21*), making them potentially useful minimally perturbing probes of *in situ* domain orientation. No structure exists for a similar mutant in the regulatory domain of TnC, nor have any of these mutations been characterized in terms of their interactions with the appropriate target regions of TnI. At the highest level, it is important to characterize the physiological activity (i.e., force development) of these proteins when reconstituted into muscle fibers.

The focus of this paper is the biophysical characterization and structure determination of the calcium binding site II mutant F77W in the regulatory domain of cTnC. In the course of this work, we discovered by NMR that we had unintentionally expressed the double mutant F77W-V82A-cNTnC. Consequently, the calcium and cTnI switch peptide (cSp) affinities were studied for both F77W and F77W-V82A-cNTnC in this paper, as well as the determination of the three-dimensional solution structure of F77W-V82A-cNTnC•Ca^{2+} using multinuclear, multidimensional NMR spectroscopy. Finally, we present the *in situ* force recovery (activity) of all of the Phe-to-Trp mutants reconstituted in skeletal muscle fibers, including 4*f*W and 5*f*W analogues. The results revealed a correlation between the structural changes introduced by the tryptophan mutation in the regulatory N-domain, the affinity changes for the binding of the 'switch' region of cTnI, and the concomitant changes in the maximal force developed *in situ* in muscle fibers. No such perturbation is observed for the mutations made in the C-terminal domain of cTnC, consistent with its stronger interactions with cTnI and its structural role in the mechanism.

MATERIALS AND METHODS

Protein and Peptide Nomenclature. Full length human cardiac troponin C is referred to as cTnC (residues 1−161). The N-domain and C-domain of cTnC are referred to as cNTnC (residues 1−89) and cCTnC (residues 91−161). The Phe-to-Trp mutation at position 77 in cTnC is referred to as F77W-cTnC for the full length and F77W-cNTnC for the N-domain. cTnC containing the mutations Phe 77 to Trp and Val 82 to Ala is referred to as F77W-V82A-cTnC for the full length protein and F77W-V82A-cNTnC for the N-domain. The human cardiac troponin I is referred to as cTnI. The specific region of cTnI containing residues 147−163 is referred to as $cTnI_{147-163}$ or cSp (cardiac switch peptide): (Ac)-RISADAMMQALLGARAK-(amide).

Protein Expression and Purification of TnC and cNTnC Mutants. The plasmid DNA pET3a-F77W-cNTnC (1−89), pET3a-F77W-V82A-cNTnC (1−89), pET3a-F77W-cTnC (1−161) and pET3a-F77W-V82A-cTnC (1−161) were used to transform BL21(DE3)pLysS cells. The expressions of unlabeled, {^{15}N}-labeled, and {^{15}N, ^{13}C}-labeled protein in *E. coli* were as described by Gagné et al. (*22*) and Li et al. (*23*). Purification of the proteins followed the previously published protocol for TnC. Decalcification was done as described by Li et al. (*23*).

Calcium Titrations. The calcium binding affinity of cNTnC, F77W-cNTnC, and F77W-V82A-cNTnC were measured via competition with a chromophoric chelator. Ca^{2+}-free buffer (100 mM KCl, 50 mM MOPS, pH = 7.5) was prepared as described by Linse (*24*). The calcium binding affinity of the chromophoric chelator (BAPTA) was measured at $\lambda = 238.5$ nm ($K_d = 0.5 \pm 0.3$ μM, $n = 5$). The binding constant of each protein was then determined by calcium titration of the protein in presence of BAPTA. The absorbance changes were verified to come from the chelator only at the wavelength specified above. The protein concentrations (from amino acid analysis) were kept as close as possible to the chelator concentration used: BAPTA (44 μM), cNTnC (48 μM), F77W-cNTnC (45 μM), and F77W-V82A-cNTnC (50 μM). The calcium binding constants of the proteins were extracted from the fitting of the normalized absorbance at each point of titration plotted as a function of the calcium concentration, using an in-house script, following the procedures outlined by Linse (*24*).

cSp Titrations. A 1.0 mg amount of ^{15}N-labeled protein was dissolved in 550 μL of NMR buffer (90% H_2O:10% D_2O and 100 mM KCl) for a final protein concentration of 0.1 mM (from amino acid analysis). To the sample were added $CaCl_2$ (5.0 mM), DTT (12.5 mM), 0.03% sodium azide, and protease inhibitors to prevent sample degradation. DSS was added to reference the spectra. The pH was adjusted to 6.8 according to the imidazole signal from the 1D spectrum. A 2D {^{1}H−^{15}N}-HSQC, with 512 (t_2) × 128 (t_1) complex points, was acquired for every of step of the cSp titration. Solid peptide was weighed and added directly into the NMR sample at every step; cSp has insufficient water solubility to allow the preparation of a solution stock concentrated. The following cSp concentrations were used for F77W-V82A-cNTnC: 0.00, 0.10, 0.20, 0.31, 0.42, 0.51, 0.60, 0.77, 1.01, 1.41, 2.29, and 3.70 mM of cSp. For F77W-cNTnC: 0.00, 0.10, 0.23, 0.37, 0.52, 0.69, 1.03, 1.51, 3.11, 5.77 mM of cSp. The spectra were acquired on a Varian INOVA 600 MHz spectrometer.

^{15}N-Relaxation Measurements. A 1 mg amount of ^{15}N-labeled protein was diluted in 550 μL of NMR buffer. Deuterated-DSS, DTT (12.5 mM), $CaCl_2$ (5 mM), 0.03% of sodium azide, and protease inhibitors were also added. The pH was adjusted to 6.84 according to the imidazole signal. The protein concentration was determined to be 0.2 mM from an amino acid analysis. For both samples, the ^{15}N-transverse relaxation rates were measured by acquiring six 2D {^{1}H−^{15}N}-HSQC NMR spectra using the BioPack pulse sequence with different relaxation time delays (τ = 10, 30, 50, 70, 90, 110 ms). To measure the ^{15}N-longitudinal relaxation rates,

Table 1: Structural Statistics of F77W-V82A-cNTnC·Ca^{2+} (30 Structures)

NOE restraints	1250
short range ($\|i-j\|=1$)	734
medium range ($1<\|i-j\|<5$)	333
long range ($\|i-j\|\geq 5$)	183
calcium binding restraints	8
dihedral angle restraints from TALOS	152
Φ	76
Ψ	76
coupling constants	58
distances violations (no.)[a]	12
Ramachandran plot for residues 1−89[b]	
Φ/Ψ in most favored region	91.6%
Φ/Ψ in additionally allowed region	8.4%
Φ/Ψ in generously allowed region	0.0%
Φ/Ψ in disallowed region	0.0%
atomic rmsd (Å)[c]	
backbone atoms (N, Cα, C′)	0.67 ± 0.16
heavy atoms	1.16 ± 0.12

[a] Violated in >10 structures. No violations >0.4 Å. [b] Calculated with PROCHECK_NMR v.3.5.4, excluding GLY and PRO. [c] Calculated with CYANA over residues 5−85.

seven {^{1}H−^{15}N}-HSQC spectra were acquired with the following time delays: τ = 10, 50, 100, 200, 300, 500 and 800 ms. The {^{1}H−^{15}N}-HSQC spectra were all collected with 512 (t_2) × 128 (t_1) complex points and the relaxation delay between pulse sequences was set to 3.0 s. The spectra were acquired on a Varian INOVA 600 MHz NMR spectrometer.

Data Acquisition, Chemical Shift Assignments, and NMR Restraints. A {^{15}N-^{13}C}-F77W-V82A-cNTnC sample was prepared similarly to the one made for the acquisition of the ^{15}N-relaxation data, but a higher protein concentration (~1.5 mM) was used in addition to 19% TFE (v/v). This sample was used to acquire the spectra needed for the chemical shift assignments and the structure determination of F77W-V82A-cNTnC·Ca^{2+}. The spectra were all processed using NMRPipe (*25*). The chemical shifts were assigned using smartnotebook v5.1.3 (*26*) and NMRView 5.2.2 (One Moon Scientific, Inc.). The following spectra were used for the chemical shift assignments: 2D-{^{1}H−^{15}N}-HSQC, 3D-{^{1}H−^{15}N}-TOCSY-HSQC, 3D-CBCACONNH, 3D-HNCACB for the backbone and 3D-CCONH, 3D-HCCONH, 3D-HCCH-TOCSY and two 2D-{^{1}H−^{13}C}-HSQC (aliphatic and aromatic) for the side chains. The structural restraints were obtained from a 3D-{^{15}N}-NOESY-HSQC and two 3D-{^{1}H−^{13}C}-NOESY-HSQC (aliphatic and aromatic) for the NOEs, and a 3D-HNHA to measure the $^3J_{HNH\alpha}$ coupling constants (phi angles).

Structure Calculation. The structure calculations were performed using CYANA 2.1 (*27*). Most of the NOEs were assigned manually and calibrated within CYANA. The noeassign procedure in cyana assigned 235 out of 1250 NOEs. The minimum and maximum NOE calibration values were set to 1.8 and 6.0 Å, respectively. The program was forced to keep all of the manually assigned NOEs for the seven runs (8000 steps) of calculation. In addition, 8 calcium binding restraints (based on calcium binding site homology), 103 dihedral restraints from TALOS (*28*), and 68 $^3J_{HNH\alpha}$ were used to obtain the NMR ensemble (see Table 1). The structure validation was performed using procheck v.3.5.4. (*29*). No further refinement was necessary in order to obtain this well-resolved NMR ensemble.

Muscle Fibers and Solutions. Adult New Zealand white rabbits were killed by sodium pentobarbitone injection (200 mg kg^{-1}). Small fiber bundles were dissected from the psoas muscle, demembranated, and stored for up to four weeks in relaxing solution containing 50% (v/v) glycerol at −20 °C (*30*). Single fiber segments 2.5−3.5 mm long were dissected in the above storage solution on a cooled microscope stage and mounted, via aluminum T-clips, at sarcomere length 2.4 μm between a force transducer (AE801, Memscap, Bernin, France) and a fixed hook, in a 60-μL glass trough containing relaxing solution. The experimental temperature was 10.0 ± 0.5 °C. All experimental solutions used in muscle fiber experiments contained 5 mM Mg-ATP, 1 mM free Mg^{2+}, and 25 mM imidazole, except where noted. Ionic strength was adjusted to 150 mM by addition of potassium propionate (KPr), and the pH was 7.1 at 10 °C. The relaxing solution also contained 10 mM EGTA. The activating solution contained 10 mM Ca-EGTA (pCa 4.5, where pCa = −log-[Ca^{2+}]). The preactivating solution contained 0.2 mM EGTA. TnC-extraction solution contained 0.5 mM trifluoperazine (TFP), 20 mM MOPS, 5 mM EDTA, and 130 mM KPr, pH 7.1 at 10 °C.

TnC Extraction and Reconstitution. Ca-activated force prior to TnC extraction (T_0) was determined at pCa 4.5. Endogenous skeletal TnC was selectively extracted from single glycerinated rabbit psoas muscle fibers by 10 cycles of 30-s incubations in TnC-extraction solution followed by 30 s in relaxing solution (*14*). Fibers were reconstituted with cTnC by bathing them in relaxing solution containing 1−2 mg/mL cTnC for up to 20 min at 10 °C. No further increase in active force could be detected with subsequent incubations in cTnC.

RESULTS

The focus of this paper is the biochemical and structural characterization of the calcium binding site II mutant F77W in the regulatory N-domain of cTnC, and the physiological characterization of a series of Trp mutants in both the structural and regulatory domains. Calcium binding site I in cTnC is naturally defunct and flexible, and therefore the mutant F27W was not studied. Midstream in our work, we discovered by NMR that we had unintentionally expressed the double mutant F77W-V82A-cTnC. Consequently, the F77W single mutant was recloned, expressed, and labeled, and the NMR and biochemical measurements including calcium and cTnI switch peptide affinities were studied for both F77W- and F77W-V82A-cTnC. The results show that the V82A mutation has no consequence on any of the biophysical properties of the protein, which is supported by the *in situ* fiber force recovery measurements conducted on both F77W mutants. The {^{1}H−^{15}N}-2D-HSQC NMR spectra at 600 MHz of F77W- and F77W-V82A-cTnC·Ca^{2+} are presented in Figure 1. These NMR spectra were run at 100 μM protein where dimerization (see below) is negligible. Residue specific assignments are indicated. Since amide ^{1}H and ^{15}N NMR chemical shifts are very sensitive to minute changes in structure, chemical environment, and dynamics, the comparison of the spectra for F77W- and F77W-V82A-cNTnC·Ca^{2+} shows in exquisite detail on a residue specific basis that the two structures are virtually identical. Consequently the NMR structure and dynamics are presented only

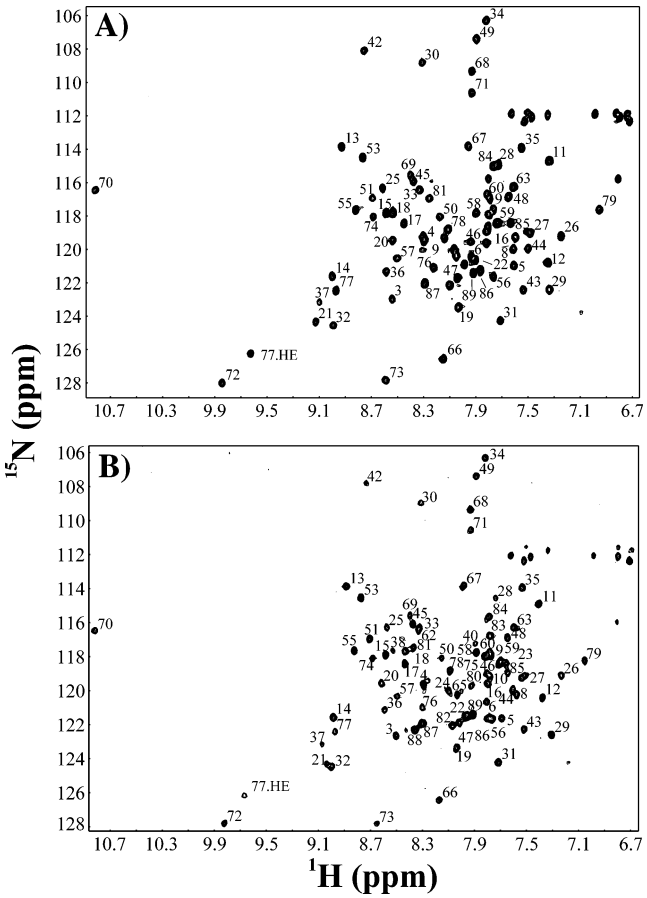

FIGURE 1: {^{1}H−^{15}N}-2D-HSQC NMR spectra at 600 MHz of (A) F77W-cNTnC·Ca^{2+} and (B) F77W-V82A-cNTnC·Ca^{2+} showing the very close similarity between both F77W mutants. The numeric labels indicate the residue specific assignments.

for F77W-V82A-cTnC·Ca^{2+} since replication would provide little addition information.

Dimerization of the N-Domain of Troponin C. It is known that the N-domain of TnC dimerizes weakly in solution at typical NMR concentrations, and that the tendency to dimerize is greater for skeletal than cardiac NTnC (K_{dimer} = 1.3 vs 7.3 mM, respectively) (*31*). To evaluate the monomer: dimer equilibria for F77W- and F77W-V82A-cNTnC·Ca^{2+}, we measured backbone amide ^{15}N-R_2 relaxation rates as a function of protein concentration ranging from 0.11 to 3.4 mM. Several peaks were impossible to identify at higher concentrations but appeared as unambiguous resonances at low concentration. This is the result of extensive exchange broadening of the NMR cross-peaks. Analysis of the data gave a K_{dimer} of approximately 5 mM for both proteins, indicating that the mutation V82A is not responsible for the increase of dimerization. The increased dimerization reflects a more open structure and exposed hydrophobic domain (see below). Since the weak dimerization affects the observed calcium and ligand affinities, all interactions for both proteins were studied at low protein concentrations. Multinuclear 3D NMR structural data was collected at higher concentrations in the presence of the cosolvent TFE, used as a denaturant of quaternary structure (*5*, *32*).

Calcium and cSp Affinities of F77W Mutants. Calcium and cSp affinities of both mutants were measured to determine whether the presence of the Trp disturbs the interaction with calcium, the coupled 'closed' to 'open' conformational equilibrium, or the subsequent binding of cTnI in the hydrophobic pocket of the calcium-saturated cNTnC. The calcium dissociation constants were measured using an optical method in which the apparent calcium binding affinity of the chromophoric chelator BAPTA is measured in the absence and presence of the calcium binding protein, and the difference attributed to competition from binding to the protein. These measurements are performed at protein concentrations <50 μM where dimerization is negligible (data not shown). A K_d of 4 ± 3 μM was obtained for wild type cNTnC, and K_ds of 15 ± 5 and 18 ± 5 μM for the mutants F77W and F77W-V82A, respectively.

The cSp affinity of both mutants were measured by following the chemical shift changes of the amide resonances in {^{1}H−^{15}N}-2D-HSQC NMR spectra of cNTnC·Ca^{2+} acquired during titration with cSp. These NMR spectra were run at 100 μM protein concentration where dimerization is negligible. This also allows for the asymptote of the titration to be well defined, resulting in an accurate determination of the dissociation constants. The cSp titrations for F77W- and F77W-V82A-cNTnC·Ca^{2+} are shown as overlay NMR plots in Figure 2. The comparison of the spectra at the beginning and end of both titrations shows that nearly identical structural changes occur in both proteins upon cSp binding. Seven residues showing unambiguous chemical shifts in both cSp titrations were followed: Ala31, Glu66, Gly30, Gly42, Leu29, Ser37, and Thr71. The average chemical shift changes $[\sqrt{(\Delta\delta_{1H})^2 + (0.2\ \Delta\delta_{15N})^2}]$ were plotted as a function of the ratio of the total cSp concentration over the protein concentration (see inserts Figure 2). A K_d of 456 ± 35 μM was measured for the mutant F77W-V82A-cNTnC·Ca^{2+} and a K_d of 470 ± 35 μM for F77W-cNTnC·Ca^{2+}. Those values are three times higher than the K_d obtained by Li et al. (*33*) for cNTnC (154 ± 10 μM), demonstrating the weaker affinity of the Phe-to-Trp mutants for cTnI.

Characterization of the Dynamics of F77W-V82A-cNTnC·Ca^{2+}. The backbone amide ^{15}N-relaxation rates (^{15}N-R_1 and ^{15}N-R_2) of F77W-V82A-cNTnC·Ca^{2+} were determined on a per residue basis at a protein concentration of 200 μM (Figure 3). The comparison of those relaxation rates with the ones observed by Spyracopoulos et al. (*34*) for the wild type protein does not reveal any major differences in the profile of R_1 and R_2 values: the N- and C-termini are more flexible than the rest of the protein (low R_1 and R_2), the defunct calcium binding site I is also more flexible than the functional binding site II, and the secondary structures in general are more stable than the loop regions (as judged by the R_1/R_2 ratios). We obtained an average ^{15}N-R_1 of 2.5 ± 0.4 s^{-1} (cNTnC: 2.3 ± 0.6 s^{-1}) and ^{15}N-R_2 of 9.4 ± 0.8 s^{-1} (cNTnC: 6.5 ± 1.3 s^{-1}) for all characterized residues (n = 79). The average ^{15}N-R_2 drops to 7.9 ± 0.4 s^{-1} if the seven ^{15}N-R_2 values higher than 15 s^{-1} are excluded. We measured similar relaxation rates for mutant F77W-cNTnC (data not shown). The lower average transverse relaxation rate measured for the Trp mutants is due to residual dimerization in solution.

Structure of F77W-V82A-cNTnC·Ca^{2+} in TFE. The structure of the mutant F77W-V82A-cNTnC·Ca^{2+} was determined by NMR in the presence of 19% TFE (v/v). The cosolvent TFE is used here as a denaturant of quaternary structure to reduce dimerization (*5*, *32*). and was shown to not modify

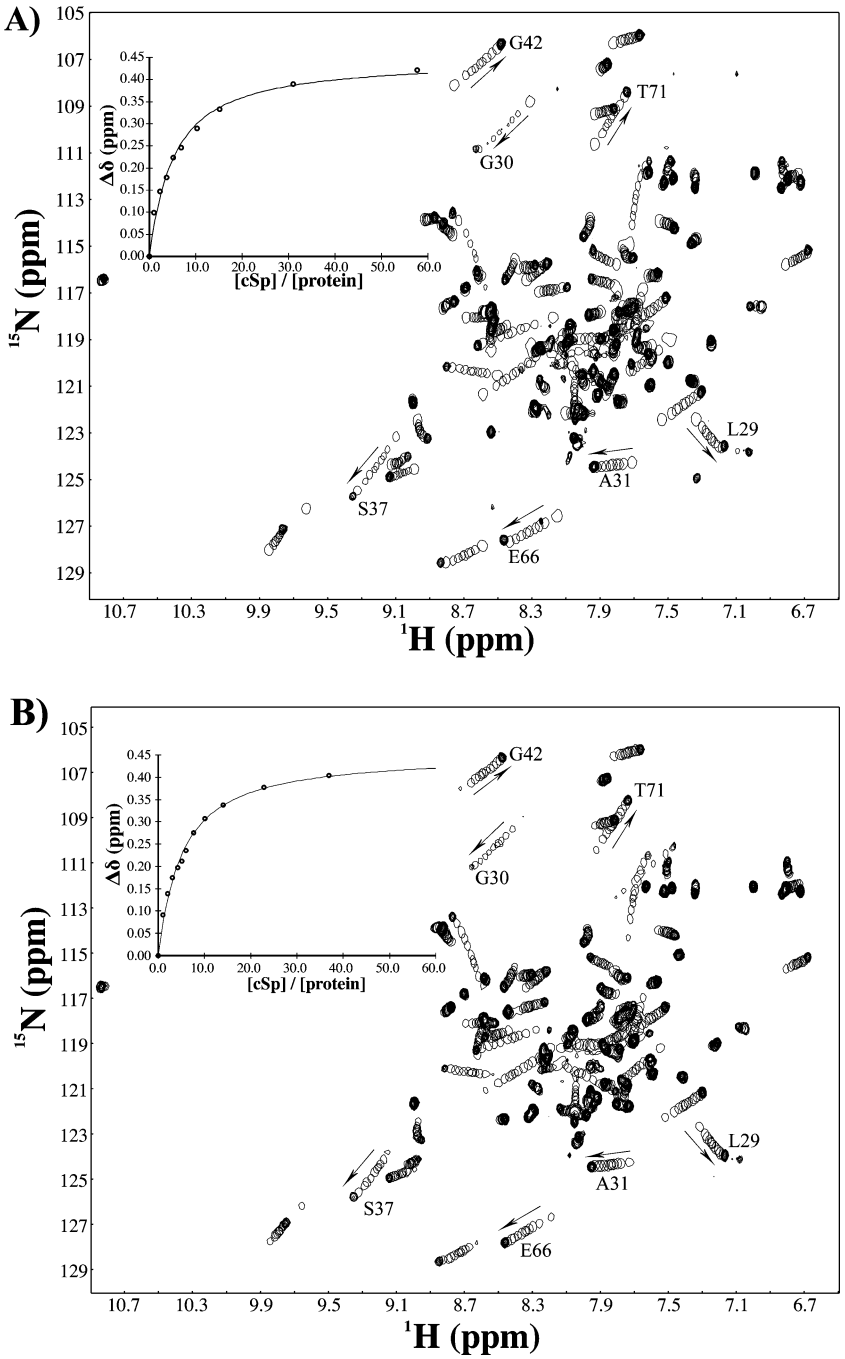

FIGURE 2: cSp titrations of F77W and F77W-V82A-cNTnC·Ca^{2+} performed at a low concentration of protein (~0.1 mM). The seven labeled residues were used to measure an average chemical shift change for each step of the titrations. Inset: the chemical shift changes are plotted as a function of the [cSp]/[protein] ratio, and the best fit is represented by a continuous line. A K_d of 470 ± 47 μM was measured for mutant F77W (A) and 456 ± 35 μM for mutant F77W-V82A (B).

the structure of cNTnC·Ca^{2+} by comparison of the NMR structures determined without (*34*) and with TFE (*32*). The NMR ensemble of F77W-V82A-cNTnC·Ca^{2+} containing the 30 structures with lowest rmsd (out of 50) is presented in Figure 4A. All of the structures in the ensemble have a good protein geometry with 91.6% of the dihedral angles in the most favorable region of the Ramachandran plot and 8.4% in the additionally allowed region (Table 1). The backbone rmsd is 0.67 ± 0.16 Å, and 1.16 ± 0.12 Å for the heavy atoms. There are no NOE violations more than 0.4 Å. Overall, the mutations F77W and V82A do not change the structure of cNTnC. The protein shows two EF-hand motifs. The calcium binding site I is still structured, and its overall structure is unchanged. The length and sequential position of the secondary structures are identical: N-helix (5−11), A-helix (14−27), B-helix (41−48), C-helix (54−62), D-helix (74−84), and the small β-sheet (35−37, 71−73). The superimposition of F77W-V82A-cNTnC onto cNTnC (1AP4) shows a rmsd of 2.4 Å (Figure 4B) for the backbone atoms of the secondary structures (N, Cα, C′). Residue 77 of the two structures is represented in sticks, confirming that both aromatic rings share the same position in the hydrophobic core of the N-domain of TnC.

Even though the overall fold of the protein is conserved, the structure of F77W-V82A-cNTnC·Ca^{2+} reveals two significant changes. First, a comparison of this Trp mutation

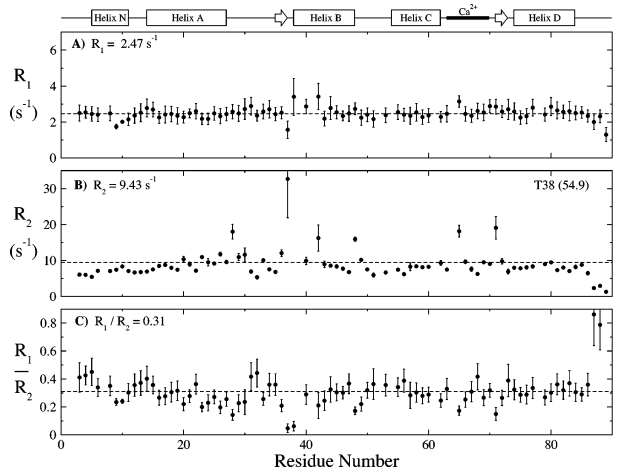

FIGURE 3: ^{15}N-Relaxation of F77W-V82A-cNTnC·Ca^{2+} at ~0.2 mM. The ^{15}N-R_1, ^{15}N-R_2, and R_1/R_2 ratio are plotted as a function of the primary sequence on a per residue basis with their respective error bars. The averages for the three relaxation values are shown with dashed lines.

in cNTnC with other Trp mutation in homologous proteins revealed that the indole ring of F77W is in the opposite/antiparallel orientation (see Discussion section). Second, the F77W mutation, replacing a phenyl side chain by a larger indole ring, has created a more open conformation than for cNTnC. We have measured the interhelical angles between helix A and B, and between C and D, for F77W-V82A-cNTnC and cNTnC in the presence or absence of the cSp (PDB 1ap4 and 1mxl) using interhlx (K. Yap, University of Toronto). The interhelical angles A/B and C/D are a good indication of the opening of the N-domain of cTnC. A decrease in the interhelical angle indicates an opening of the structure. Interestingly, interhelical angle values from F77W-V82A-cNTnC·Ca^{2+} (A/B = 112°, B/C = 93°) are similar to those found in cNTnC·Ca^{2+}·$TnI_{147-163}$ (A/B = 105°; C/D = 89°) but different from the wild type cNTnC·Ca^{2+} (A/B = 132°; C/D = 122°). Furthermore, the structural superimposition of F77W-V82A-cNTnC·Ca^{2+} with cNTnC·Ca^{2+}·$TnI_{147-163}$ (Figure 5A) has a lower rmsd (2.1 Å) than when the structure is superimposed on cNTnC·Ca^{2+} (2.4 Å) using the backbone atoms of the secondary structures (N, Cα, C′). All these comparisons demonstrate that the insertion of a Trp in the core of the N-domain of cTnC generates a more open structure, similar to wild type cNTnC·Ca^{2+}, but even more to cNTnC·Ca^{2+}·$TnI_{147-163}$.

Regulation of Active Force by Trp Mutants in Skeletal Muscle Fibers. Extraction of the native skeletal TnC from single demembranated fibers of rabbit psaos muscle using trifluoperazine (see Materials and Methods) reduced the active isometric force measured in standard activating solution (pCa 4.5) to 8.7 ± 1.0% (mean ± SE, n = 29) that observed prior to TnC extraction (T_0). After reconstitution with recombinant skeletal TnC the active force recovered to 92.2 ± 4.3% of T_0 (n = 3). Force recovery after reconstitution with wild type cardiac TnC (cTnC) was only 65.4 ± 3.4% (n = 7) of T_0, similar to previously published values (65.4%, (*35*); 71%, (*36*)).

Active force recovery in fibers reconstituted with the F104-(4*f*W), F153(4*f*W), and F153(5*f*W) mutants of cTnC was 75.0 ± 6.1% (n = 4), 61.3 ± 5.8% (n = 4), and 68.2 ± 4.2% (n = 3) of T_0, respectively (Table 2), and these values are not significantly different from that reported above for wild type

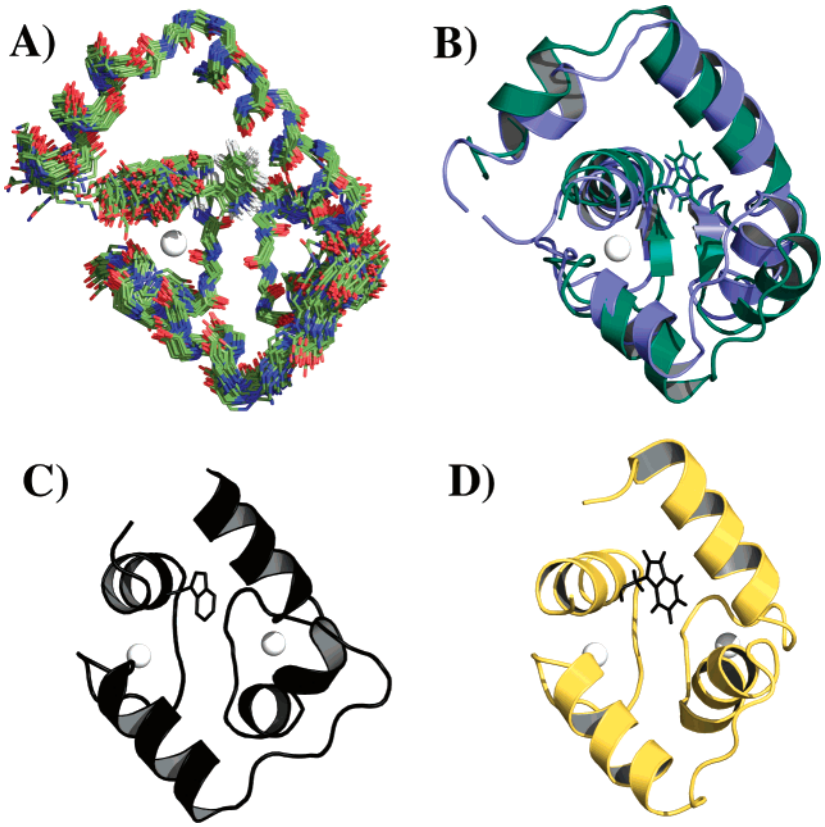

FIGURE 4: (A) NMR ensemble (30 structures) of F77W-V82A-cNTnC·Ca^{2+} in TFE. (B) Superposition of F77W-V82A-cNTnC and cNTnC and a comparison of the orientation of both residues 77 (W77 vs F77). Structural comparison with (C) silver hake parvalbumin (X-ray) and (D) cCTnC mutant F153W (NMR) with their respective Trp residue represented with sticks.

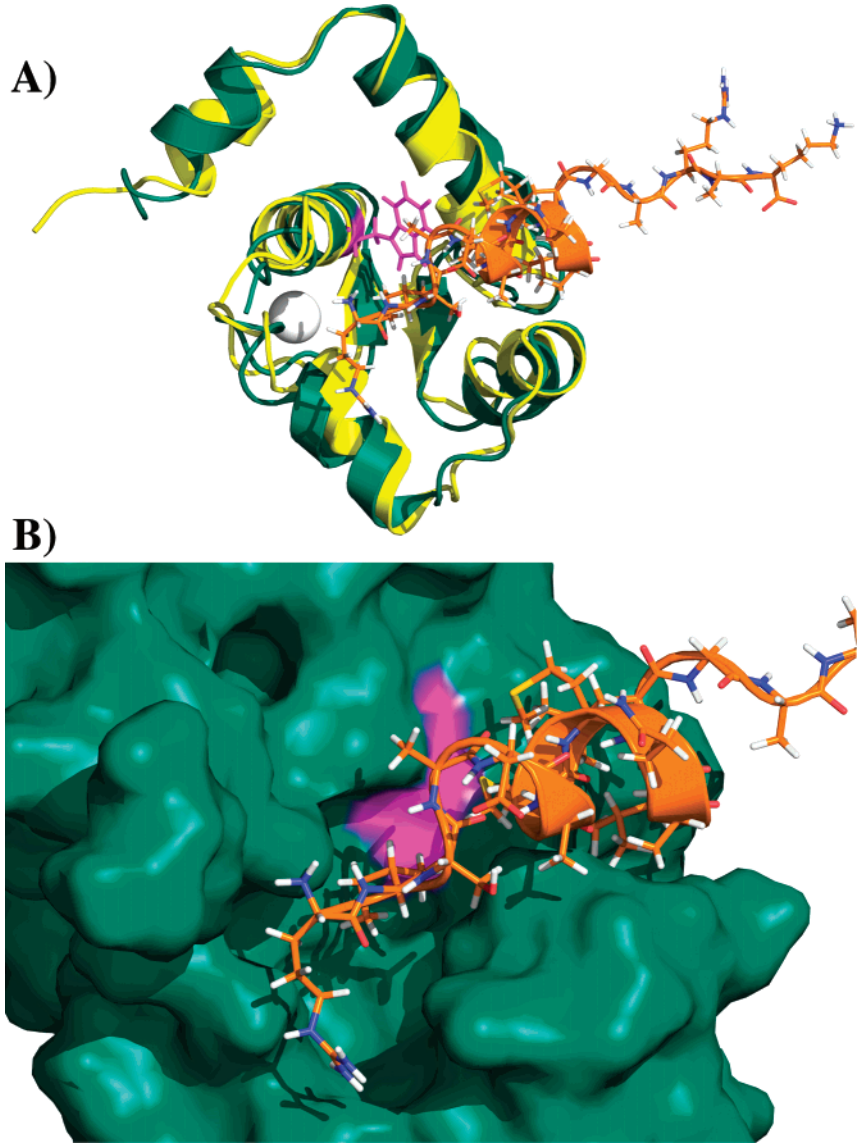

FIGURE 5: (A) Superposition of F77W-V82A-cNTnC·Ca^{2+} (green) and cNTnC·Ca^{2+}·cSp (yellow) structures both determined by NMR. The Trp77 of the mutant is colored in pink and the cSp bound to the wild type is colored in orange. (B) Potential interaction of cSp with F77W-V82A-cNTnC·Ca^{2+}. The figure was created using the same orientation as in A. The green surface corresponds to the surface area of F77W-V82A-cNTnC with residue Trp77 colored in pink.

Table 2: Active Force at pCa 4.5 after Reconstitution with cTnC (% of the maximal force observed prior to extraction)[a]

human cTnC	active force (% T_0)	no. of experiments
F104 (4F-Trp)	75.0 ± 6.1	4
F153 (4F-Trp)	61.3 ± 5.8	4
F153 (5F-Trp)	68.2 ± 4.2	3
F77W	40.0 ± 5.5*	4
F77W-V82A	39.6 ± 4.5*	5
wild type	65.4 ± 4.3	7

[a] Mean ± SEM; *$P < 0.01$ when compared with wild type.

cTnC ($P > 0.05$). Fibers were fully relaxed at pCa 9.0 after TnC extraction and after reconstitution with the F104(4*f*W), F153(4*f*W), and F153(5*f*W) mutants of cTnC. Thus, the introduction of 4*f*W or 5*f*W at either of these sites in the C-terminal lobe of cTnC has no effect on Ca^{2+}-regulation in muscle fibers beyond that associated with replacement of TnC by cTnC. In contrast, active force recovery in fibers reconstituted with the F77W and F77W-V82A mutants of cTnC was only 40.0 ± 5.5% ($n = 4$) and 39.6 ± 4.5% ($n = 5$), respectively, significantly lower than that observed for wild type cTnC ($P < 0.01$). Moreover, the fibers containing F77W- and F77W-V82A-cTnC were not completely relaxed at pCa 9.0 but generated a force of 2.8 ± 0.3% of T_0. Thus, introduction of Trp at these sites in the N-terminal lobe of cTnC does affect Ca^{2+} regulation *in situ*. The decrease in active force in fibers reconstituted with cTnCs is unlikely to be due to incomplete occupation of the TnC binding sites in the fiber, because an additional 5 min incubation with recombinant skeletal TnC produced no further recovery of active force (−1.1 ± 0.9%, $n = 7$).

DISCUSSION

Ca^{2+} and cSp Affinity Measurements. We have measured the calcium binding affinities of both F77W mutants in comparison to wild type cNTnC. We obtained K_ds of 5, 15, and 18 μM for cNTnC, F77W, and F77W-V82A, respectively. The K_d for cNTnC is consistent with the previous published values (*37*, *38*). The results suggest that the mutation F77W reduces the calcium affinity of cNTnC by ~3 fold. Moncrieffe et al. (*15*) observed a 2-fold reduction

in Ca^{2+} affinity for the skeletal F154W-TnC mutant (see also (*39*)) but only a small reduction in Ca^{2+} affinity for the F78W mutant, which is the skeletal analogue to F77W. The cSp binding affinity of mutants F77W and F77W-V82A was also monitored by NMR at low protein concentrations. The $\{^1H-^{15}N\}$-HSQC NMR spectra at high protein concentration were of poor quality, while the high quality spectra obtained during the titrations at a lower protein concentration are presented in Figure 2. Another advantage of using low protein concentrations in our binding affinity measurements is that as high as 40- to 60-fold molar excess of [cSp] over [protein] is possible. This is not possible at higher protein concentrations because of limited peptide solubility. This allows one to reach a plateau in the chemical shift changes, which is reflected in a much more accurate and precise determination of the dissociation constant. The cSp binding affinity of both mutants F77W and F77W-V82A are decreased by a factor 3 in comparison to wild type cNTnC. The fact that the results were similar for both mutants indicates that the mutation V82A does not affect the binding affinity of the mutants to cTnI.

Structure of F77W-V82A-cNTnC·Ca^{2+} and Trp Orientation. The solution structure of mutant F77W-V82A-cNTnC in the calcium state has been determined in the presence of TFE. The overall structure of the double mutant is very similar to that of wild type cNTnC. The side chain of Trp77 is located at the same position as Phe77 in the wild type (Figure 4B) with similar χ_1 and χ_2 values. The indole ring is well defined in the core of the protein (Figure 4A). However, a comparison of this Trp mutant in cNTnC and other Trp mutants in homologous proteins reveals an important change: the indole ring in the mutant F77W-V82A is in the opposite orientation compared to some homologous proteins. For example, the NMR structure of the F153W mutant has an indole ring orientation with the HN-bond pointing up (Figure 4D) (*21*). The mutant F153W in the C-domain shares the homologous position as F77W in the N-domain, both sharing similar χ_1 angles (F77W = 177° and F153W = 177°) but having different χ_2 angles (F77W = 90° and F153W = −96°). Silver Hake Parvalbumin has a single Trp (W102) buried in the core of its domain and in an analogous position to F77W-V82A-cNTnC and F153W-cCTnC (Figure 4C). In the X-ray structure the indole orientation is also opposite with a similar χ_1 value (W102 = 170°) but again a different χ_2 value (W102 = −106°) (*40*). The same orientation is observed in the structure of carp parvalbumin mutant F102W (*41*). Moncrieffe et al. discuss possible heterogeneity of the indole ring orientation in the context of Trp fluorescence lifetime experiments but conclude that they only observe evidence for one major conformation (>97%). Their minimum perturbation maps suggest two possible minima having similar χ_1 angles of ∼180° but different χ_2 values of approximately 100° and −100°. A similar computer simulation was performed for F78W-sNTnC, the skeletal homolog of F77W, and two energy minima were also obtained, the more stable of which corresponding to the orientation observed in F77W-V82A-cNTnC (*15*). We have also generated a model for F77W-V82A-cNTnC based on the structure of cNTnC (PDB 1AP4) using Modeler 9v1 (*42*). The ensemble of structures obtained after minimization revealed a Trp orientation that is in accordance with our NMR ensemble (data not shown).

Structural Consequences - There is no significant difference in the binding affinity of the two mutants for the cSp or Ca^{2+}. This suggests that the mutation V82A does not influence the properties of the F77W mutants. The structural characteristics expected from the Trp mutants were successfully attained: the same overall structure and an immobilized Trp ring in the core of the N-domain of cTnC. One structural difference between wild type cNTnC and mutant F77W-V82A is the larger extent of opening of the mutant. The comparison of the structures of F77W-V82A-cNTnC·Ca^{2+} with cNTnC·Ca^{2+}·cSp shows a similar opening (Figure 5A). One would expect that a more open N-domain would lead to an increase in the cSp affinity; i.e., sNTnC (more open) has a higher affinity for sSp than cNTnC (less open) has for cSp. However, the cSp binding is weaker even though the structure of the Phe-to-Trp mutant is more open. One possibility is that the Phe-to-Trp substitution makes unfavorable contacts with cTnI, as the indole ring appears at the surface of the F77W-V82A-cNTnC·Ca^{2+} structure (Figure 5B). Interestingly, the HN resonance of the Trp indole disappears from the $\{^1H-^{15}N\}$-HSQC NMR spectrum after the first step of the cSp titration and does not reappear even after an addition of more than a 40-fold molar excess of peptide. This indicates that the chemical environment of the Trp is highly modified by the presence of the cSp, supporting the interpretation of a direct contact between Trp77 and cTnI.

Force Recovery of Different Phe-to-Trp Mutants. Similarly to the cSp and Ca^{2+} binding affinities discussed above, the recovery of force in reconstituted skeletal muscle fibers is about the same for the F77W- and F77W-V82A mutants, indicating once again that the V82A mutation is benign. The force recovery profiles for the F104W (site III) and F153W (site IV) are similar and not significantly different from wild type cTnC, which is used as a control in the skeletal muscle fibers. However, the force recovery for the F77W and F77W V82A (site II) and F153W mutants are much less than that of the wild type cTnC. This is consistent with the expected structural role of the C-domain and the expected regulatory role for the N-domain derived from the large body of existing studies. At a molecular level, the insensitivities of muscle function to C-domain Phe-to-Trp mutations indicate that either the Phe-to-Trp mutations do not affect TnC−TnI interaction, or the change in affinity of cCTnC for cTnI is not enough to compromise the anchoring of TnI to TnC in the troponin complex. For F77W, the mutation reduced cTnC's affinity for cSp, thus attenuating the critical Ca^{2+}-dependent interaction responsible for triggering muscle contraction. This is directly reflected in the change in recovery of force. One qualification of these studies would be that the interaction in the reconstituted fibers is with sSp and not cSp, but their sequences are very similar and critical residues such as M154 are identical between the two. The sequence of $cSp_{147-163}$ is RISADAMMQALLGARAK, and that of $sSp_{115-131}$ is RMSADAMLRALLGSKHK. In some fibers, chicken skeletal TnC was also used after reconstitution with human cardiac TnC and no further force recovery was observed, indicating that the incomplete reconstitution of cTnC could be ruled out as the reason for the incomplete force recovery after reconstitution with human cardiac TnC.

The overall conclusions of this study are that while the Phe-to-Trp mutations in cNTnC studied cause only relatively small changes at the level of molecular structure, the effect

can be to perturb the interactions with target proteins, and this is then reflected at the level of force generation when reconstituted into fibers. Further, the effects of the Phe-to-Trp mutations are differential: those in the C-lobe do not result in any change in activity, consistent with its role as a structural anchor, whereas those in the N-lobe, while small, are critical to activity since they directly regulate the Ca^{2+} signaling. A reduction in affinity between regions of cTnC and cTnI of only 3-fold leads to a 30% reduction in physiological activity. Thus, we can begin to correlate interactions now understood at a 3D structural level with the resulting downstream effects on function. At present considerable effort is being spent investigating the influence of familial hypertrophic cardiomyopathy mutations on cardiac muscle performance. Our study indicates that even the very small changes in biophysical properties that are observed can have a significant effect on long-term function.

ACKNOWLEDGMENT

The authors thank the Canadian National High Field NMR Centre (NANUC) for their assistance and use of the facilities. Operation of NANUC is funded by the Canadian Institutes of Health Research, the Natural Science and Engineering Research Council of Canada and the University of Alberta. We thank Melissa L. Rakovszky for protein expression and purification, Craig Marvin and Monica X. Li for their technical assistance, Ryan M. B. Hoffman and Robert Boyko for computer assistance, and Jeffrey S. DeVries for the spectrometers maintenance. The authors are also grateful to Professors Leo Spyracopoulos and David Trentham for helpful discussions. A special thanks to Dr. Pascal Mercier for his help with structure calculations.

REFERENCES

1. Sundaralingam, M., Bergstrom, R., Strasburg, G., Rao, S. T., Roychowdhury, P., Greaser, M., and Wang, B. C. (1985) Molecular structure of troponin C from chicken skeletal muscle at 3-angstrom resolution, *Science 227*, 945−948.
2. Houdusse, A., Love, M. L., Dominguez, R., Grabarek, Z., and Cohen, C. (1997) Structures of four Ca2+-bound troponin C at 2.0 A resolution: further insights into the Ca2+-switch in the calmodulin superfamily, *Structure 5*, 1695−1711.
3. Gagné, S. M., Tsuda, S., Li, M. X., Smillie, L. B., and Sykes, B. D. (1995) Structures of the troponin C regulatory domains in the apo and calcium-saturated states, *Nat. Struct. Biol. 2*, 784−789.
4. Sia, S. K., Li, M. X., Spyracopoulos, L., Gagné, S. M., Liu, W., Putkey, J. A., and Sykes, B. D. (1997) Structure of cardiac muscle troponin C unexpectedly reveals a closed regulatory domain, *J. Biol. Chem. 272*, 18216−18221.
5. Slupsky, C. M., Kay, C. M., Reinach, F. C., Smillie, L. B., and Sykes, B. D. (1995) Calcium-induced dimerization of troponin C: mode of interaction and use of trifluoroethanol as a denaturant of quaternary structure, *Biochemistry 34*, 7365−7375.
6. Herzberg, O., Hayakawa, K., and James, M. N. (1984) Crystallographic data for troponin C from turkey skeletal muscle, *J. Mol. Biol. 172*, 345−346.
7. Sykes, B. D. (2003) Pulling the calcium trigger, *Nat. Struct. Biol. 10*, 588−589.
8. Li, M. X., Wang, X., and Sykes, B. D. (2004) Structural based insights into the role of troponin in cardiac muscle pathophysiology, *J. Muscle Res. Cell Motil. 25*, 559−579.
9. Takeda, S., Yamashita, A., Maeda, K., and Maeda, Y. (2003) Structure of the core domain of human cardiac troponin in the Ca(2+)-saturated form, *Nature 424*, 35−41.
10. Vinogradova, M. V., Stone, D. B., Malanina, G. G., Karatzaferi, C., Cooke, R., Mendelson, R. A., and Fletterick, R. J. (2005) Ca-(2+)-regulated structural changes in troponin, *Proc. Natl. Acad. Sci. U.S.A. 102*, 5038−5043.
11. Corrie, J. E. T., Brandmeier, B. D., Ferguson, R. E., Trentham, D. R., Kendrick-Jones, J., Hopkins, S. C., van der Heide, U. A., Goldman, Y. E., Sabido-David, C., Dale, R. E., Criddle, S., and Irving, M. (1999) Dynamic measurement of myosin light-chain-domain tilt and twist in muscle contraction, *Nature 400*, 425−430.
12. Ferguson, R. E., Sun, Y. B., Mercier, P., Brack, A. S., Sykes, B. D., Corrie, J. E., Trentham, D. R., and Irving, M. (2003) In situ orientations of protein domains: troponin C in skeletal muscle fibers, *Mol. Cell 11*, 865−874.
13. Pirani, A., Vinogradova, M. V., Curmi, P. M., King, W. A., Fletterick, R. J., Craig, R., Tobacman, L. S., Xu, C., Hatch, V., and Lehman, W. (2006) An atomic model of the thin filament in the relaxed and Ca2+-activated states, *J. Mol. Biol. 357*, 707−717.
14. Sun, Y. B., Brandmeier, B., and Irving, M. (2006) Structural changes in troponin in response to Ca2+ and myosin binding to thin filaments during activation of skeletal muscle, *Proc. Natl. Acad. Sci. U.S.A. 103*, 17771−17776.
15. Moncrieffe, M. C., Eaton, S., Bajzer, Z., Haydock, C., Potter, J. D., Laue, T. M., and Prendergast, F. G. (1999) Rotational and translational motion of troponin C, *J. Biol. Chem. 274*, 17464−17470.
16. She, M., Dong, W. J., Umeda, P. K., and Cheung, H. C. (1998) Tryptophan mutants of troponin C from skeletal muscle−an optical probe of the regulatory domain, *Eur. J. Biochem. 252*, 600−607.
17. Gryczynski, I., Malak, H., Lakowicz, J. R., Cheung, H. C., Robinson, J., and Umeda, P. K. (1996) Fluorescence spectral properties of troponin C mutant F22W with one-, two-, and three-photon excitation, *Biophys. J. 71*, 3448−3453.
18. Pearlstone, J. R., Borgford, T., Chandra, M., Oikawa, K., Kay, C. M., Herzberg, O., Moult, J., Herklotz, A., Reinach, F. C., and Smillie, L. B. (1992) Construction and characterization of a spectral probe mutant of troponin C: application to analyses of mutants with increased Ca^{2+} affinity, *Biochemistry 31*, 6545−6553.
19. Grage, S. L., Wang, J., Cross, T. A., and Ulrich, A. S. (2002) Solid-state 19F-NMR analysis of 19F-labeled tryptophan in gramicidin A in oriented membranes, *Biophys. J. 83*, 3336−3350.
20. Correa, F., and Farah, C. S. (2005) Using 5-hydroxytryptophan as a probe to follow protein-protein interactions and protein folding transitions, *Protein Pept. Lett. 12*, 241−244.
21. Wang, X., Mercier, P., Letourneau, P. J., and Sykes, B. D. (2005) Effects of Phe-to-Trp mutation and fluorotryptophan incorporation on the solution structure of cardiac troponin C, and analysis of its suitability as a potential probe for in situ NMR studies, *Protein Sci. 14*, 2447−2460.
22. Gagné, S. M., Tsuda, S., Li, M. X., Chandra, M., Smillie, L. B., and Sykes, B. D. (1994) Quantification of the calcium-induced secondary structural changes in the regulatory domain of troponin-C, *Protein Sci. 3*, 1961−1974.
23. Li, M. X., Gagné, S. M., Tsuda, S., Kay, C. M., Smillie, L. B., and Sykes, B. D. (1995) Calcium binding to the regulatory N-domain of skeletal muscle troponin C occurs in a stepwise manner, *Biochemistry 34*, 8330−8340.
24. Linse, S. (2002) Calcium binding to proteins studied via competition with chromophoric chelators, *Methods Mol. Biol. 173*, 15−24.
25. Delaglio, F., Grzesiek, S., Vuister, G. W., Zhu, G., Pfeifer, J., and Bax, A. (1995) NMRPipe: a multidimensional spectral processing system based on UNIX pipes, *J. Biomol. NMR 6*, 277−293.
26. Slupsky, C. M., Boyko, R. F., Booth, V. K., and Sykes, B. D. (2003) Smartnotebook: a semi-automated approach to protein sequential NMR resonance assignments, *J. Biomol. NMR 27*, 313−321.
27. Guntert, P. (2004) Automated NMR structure calculation with CYANA, *Methods Mol. Biol. 278*, 353−378.
28. Cornilescu, G., Delaglio, F., and Bax, A. (1999) Protein backbone angle restraints from searching a database for chemical shift and sequence homology, *J. Biomol. NMR 13*, 289−302.
29. Laskowski, R. A., Rullmannn, J. A., MacArthur, M. W., Kaptein, R., and Thornton, J. M. (1996) AQUA and PROCHECK-NMR: programs for checking the quality of protein structures solved by NMR, *J. Biomol. NMR 8*, 477−486.
30. Sabido-David, C., Brandmeier, B., Craik, J. S., Corrie, J. E. T., Trentham, D. R., and Irving, M. (1998) Steady-state fluorescence polarization studies of the orientation of myosin regulatory light

chains in single skeletal muscle fibers using pure isomers of iodoacetamidotetramethylrhodamine, *Biophys. J. 74*, 3083−3092.
31. Spyracopoulos, L. (2001) *Know your protein: effects of weak dimerization* (Jardetzky, O., and Finucane, M. D., Eds.) IOS Press, Fairfax, VA.
32. Paakkonen, K., Annila, A., Sorsa, T., Pollesello, P., Tilgmann, C., Kilpelainen, I., Karisola, P., Ulmanen, I., and Drakenberg, T. (1998) Solution structure and main chain dynamics of the regulatory domain (Residues 1−91) of human cardiac troponin C, *J. Biol. Chem. 273*, 15633−15638.
33. Li, M. X., Spyracopoulos, L., and Sykes, B. D. (1999) Binding of cardiac troponin-I147−163 induces a structural opening in human cardiac troponin-C, *Biochemistry 38*, 8289−8298.
34. Spyracopoulos, L., Gagné, S. M., Li, M. X., and Sykes, B. D. (1998) Dynamics and thermodynamics of the regulatory domain of human cardiac troponin C in the apo- and calcium-saturated states, *Biochemistry 37*, 18032−18044.
35. Morris, C. A., Tobacman, L. S., and Homsher, E. (2001) Modulation of contractile activation in skeletal muscle by a calcium-insensitive troponin C mutant, *J. Biol. Chem. 276*, 20245−20251.
36. Moreno-Gonzalez, A., Fredlund, J., and Regnier, M. (2005) Cardiac troponin C (TnC) and a site I skeletal TnC mutant alter Ca2+ versus crossbridge contribution to force in rabbit skeletal fibres, *J. Physiol. 562*, 873−884.
37. Li, M. X., Gagné, S. M., Spyracopoulos, L., Kloks, C. P., Audette, G., Chandra, M., Solaro, R. J., Smillie, L. B., and Sykes, B. D. (1997) NMR studies of Ca^{2+} binding to the regulatory domains of cardiac and E41A skeletal muscle troponin C reveal the importance of site I to energetics of the induced structural changes, *Biochemistry 36*, 12519−12525.
38. Hazard, A. L., Kohout, S. C., Stricker, N. L., Putkey, J. A., and Falke, J. J. (1998) The kinetic cycle of cardiac troponin C: calcium binding and dissociation at site II trigger slow conformational rearrangements, *Protein Sci. 7*, 2451−2459.
39. Chandra, M., McCubbin, W. D., Oikawa, K., Kay, C. M., and Smillie, L. B. (1994) Ca^{2+}, Mg^{2+}, and troponin I inhibitory peptide binding to a Phe-154 to Trp mutant of chicken skeletal muscle troponin C, *Biochemistry 33*, 2961−2969.
40. Richardson, R. C., King, N. M., Harrington, D. J., Sun, H., Royer, W. E., and Nelson, D. J. (2000) X-Ray crystal structure and molecular dynamics simulations of silver hake parvalbumin (Isoform B), *Protein Sci. 9*, 73−82.
41. Moncrieffe, M. C., Juranic, N., Kemple, M. D., Potter, J. D., Macura, S., and Prendergast, F. G. (2000) Structure-fluorescence correlations in a single tryptophan mutant of carp parvalbumin: solution structure, backbone and side-chain dynamics, *J. Mol. Biol. 297*, 147−163.
42. Sali, A., and Blundell, T. L. (1993) Comparative protein modelling by satisfaction of spatial restraints, *J. Mol. Biol. 234*, 779−815.

BI702056G